Bioorganic Chemistry 85 (2019) 209–220

Contents lists available at ScienceDirect

Bioorganic Chemistry

journal homepage: www.elsevier.com/locate/bioorg

Identification of 1,2,4-triazoles as new thymidine phosphorylase inhibitors: Future anti-tumor drugs

Sohail Anjum Shahzad[a,*], Muhammad Yar[b,*], Zulfiqar Ali Khan[c], Lubna Shahzadi[b], Syed Ali Raza Naqvi[c], Adeem Mahmood[d], Sami Ullah[a], Ahson Jabbar Shaikh[a], Tauqir Ali Sherazi[a], Adebayo Tajudeen Bale[a], Jędrzej Kukułowicz[e], Marek Bajda[e]

[a] Department of Chemistry, COMSATS University Islamabad, Abbottabad Campus, Abbottabad 22060, Pakistan
[b] Interdisciplinary Research Center in Biomedical Materials, COMSATS University Islamabad, Lahore Campus, Lahore 54000, Pakistan
[c] Department of Chemistry, Government College University, Faisalabad 38000, Pakistan
[d] Department of Chemistry, College of Science, King Saud University, Riyadh 11451, Saudi Arabia
[e] Department of Physicochemical Drug Analysis, Faculty of Pharmacy, Jagiellonian University Medical College, 30-688 Cracow, Medyczna 9, Poland

ARTICLE INFO

Keywords:
1,2,4-Triazoles
Thymidine phosphorylase inhibitors
Antiangiogenic activity

ABSTRACT

Thymidine phosphorylase (TP) is over expressed in several solid tumors and its inhibition can offer unique target suitable for drug discovery in cancer. A series of 1,2,4-triazoles **3a–3l** has been synthesized in good yields and subsequently inhibitory potential of synthesized triazoles **3a–3l** against thymidine phosphorylase enzyme was evaluated. Out of these twelve analogs five analogues **3b**, **3c**, **3f**, **3l** and **3l** exhibited a good inhibitory potential against thymidine phosphorylase. Inhibitory potential in term of IC_{50} values were found in the range of 61.98 ± 0.43 to 273.43 ± 0.96 μM and 7-Deazaxanthine was taken as a standard inhibitor with IC_{50} = 38.68 ± 4.42 μM. Encouraged by these results, more analogues 1,2,4-triazole-3-mercaptocarboxylic acids **4a–4g** were synthesized and their inhibitory potential against thymidine phosphorylase was evaluated. In this series, six analogues **4b–4g** exhibited a good inhibitory potential in the range of 43.86 ± 1.11–163.43 ± 2.03 μM. Angiogenic response of 1,2,4-triazole acid **4d** was estimated using the chick chorionic allantoic membrane (CAM) assay. In the light of these findings, structure activity relationship and molecular docking studies of selected triazoles to determine the key binding interactions was discussed. Docking studies demonstrate that synthesized analogues interacted with active site residues of thymidine phosphorylase enzyme through π-π stacking, thiolate and hydrogen bonding interactions.

1. Introduction

Although thymidine phosphorylase (TP; EC 2.4.2.4) plays a crucial role in pyrimidine salvage to repair RNA and DNA degradation [1] however TP mediated thymidine catabolism contributes in tumor progression by delivering carbon to the glycolytic pathway in mammalian cells [2]. Many normal tissues and cells contain TP, identified in both cytoplasm and nucleus [3]. Overexpression of TP is associated with a number of pathological conditions, for instance rheumatoid arthritis, atherosclerosis, psoriasis, and inflammatory bowel disease [4]. Enzyme TP has been considered identical to angiogenic factor platelet-derived endothelial cell growth factor (PD-ECGF) [5]. The presence of TP or PD-ECGF in cancer cells activate human endothelial cell migration and invasion by the secretion of several angiogenic factors [5–8]. These angiogenic factors promote unsolicited angiogenesis, trigger tumor angiogenesis and accelerates proliferation of endothelial cells during cancer metastasis [4,9–11]. TP catalyzes the reversible phosphorolysis of thymidine to thymine and 2-deoxy-α-D-ribose-1-phosphate [12]. The resulting byproduct 2-deoxy-α-D-ribose-1-phosphate is further dephosphorylated to 2-deoxy-D-ribose [13]. Several other thymidine derived metabolites such as 5-phospho-α-D-ribose 1-diphosphate are needed for the survival of cells [2]. On the other hand, it was also found that 2-deoxy-D-ribose is an endothelial chemoattractant and interrupt endothelial cell migration through several mechanisms [13,14]. It further provides an energy source for migrating endothelial cells and involved in the progression of tumor angiogenesis [15]. In fact, monosaccharide is considered as an angiogenesis-inducing factor and it is recognized as a potential target in the advancement of anticancer drugs [13,16].

* Corresponding authors at: Department of Chemistry, COMSATS University Islamabad, Abbottabad Campus, Abbottabad 22060, Pakistan. Tel.: 0092 992 3835916; fax: 0092 992 383441 (S.A. Shahzad); Interdisciplinary Research Center in Biomedical Materials, COMSATS University Islamabad, Lahore Campus, Lahore 54000, Pakistan (M. Yar).
E-mail addresses: sashahzad@cuiatd.edu.pk (S.A. Shahzad), drmyar@cuilahore.edu.pk (M. Yar).

https://doi.org/10.1016/j.bioorg.2019.01.005
Received 29 August 2018; Received in revised form 29 December 2018; Accepted 2 January 2019
Available online 04 January 2019
0045-2068/

Although, angiogenesis is indispensably involved in tissue repair, organ development and wound healing process but its presence becomes highly undesirable during cancer progression suggesting its role in the metastatic process. Moreover, the up-regulation of the thymidine phosphorylase enzyme has been witnessed in several human cancers and various chronic inflammatory diseases, where significant correlation was found between increased level of angiogenesis and further advancement of the disease [13].

E. coli TP was selected as a model for biological screening of compounds because of structural and active site resemblances between mammalian and *E. coli* TPs. An increased level of TP/PD-ECGF enzyme up to 10-fold in several cancerous tissue as compared to normal tissue of the same organs [17], makes it an attractive cancer chemotherapy target for inhibition of tumor angiogenesis. Small molecules-based TP inhibition could be a spectacular strategy towards cancer treatment [18,19]. Thymidine phosphorylase differentiates nucleoside analogues which can be used as potential antitumor drugs. Tipiracil, a thymidine phosphorylase inhibitor in combination with trifluridine is in phase II clinical trial for the treatment of advanced colorectal cancer [20]. Among numerous heterocyclic compounds as TP inhibitors, until now few pyrimidine analogues for instance 6-amino-5-bromouracil or 6-aminothymine [21] and purine analogues such as 7-deazaxanthine [22], 5′-*O*-tritylinosine (KIN59) [23] were termed as potent inhibitors.

The triazole based heterocyclic compounds have been well exploited for several medicinal applications displaying anti-HIV, anticancer and antibacterial activities [24–29]. Various analogues of triazoles have been identified as inhibitors of many enzymes such as dihydrofolate reductase (DHFR) inhibitors [30], anti-Alzheimer agents [31], anti-diabetic activity [32], glycogen synthase kinase-3β inhibitors with anti-depressant activity [33] and carbonic anhydrases activators [34]. Several drugs containing 1,2,4-triazole ring such as intraconazole, voriconazole and fluconazole, are being used in the treatment of various diseases [35]. Apart from above applications, these motifs have also been found active against microbial and malarial infections including analgesic/anti-inflammatory properties [36–38].

Quest of potent inhibitors of thymidine phosphorylase is very important for the treatment of various neoplastic and non-neoplastic diseases. Therefore, it will be useful to consider remarkable influence of nitrogen-based heterocycles, such as tipiracil and 7-deazaxanthine in TP inhibition as an inspiration. It is very promising to design more TP inhibitors for evaluation of their potential as anticancer agents (Fig. 1). To further advance our ongoing research for the development of unique thymidine phosphorylase inhibitors [39,40], and distinctive biological potential of triazole family encouraged us to design structural analogues of 1,2,4-triazole for the hope of finding new TP inhibitors with better TP inhibitory activity. A pyrimidine ring in 7DX, TPI and KIN59 has been changed with a phenyl substituted 1,2,4-triazole moiety to offer more flexibility to adjust within the enzyme pocket site. In the newly designed 1,2,4-triazole scaffold; however, availability of more nitrogen atoms and additional presence of polar functional groups would generate extra hydrogen bonding sites. We believe that incorporation of substituted aromatic moiety together with thiol and carboxylic acid functional groups should provide a close contact between the designed scaffold and Phe210 through additional stabilizing interactions. In present study, we report the synthesis, characterization and enzyme inhibition of 1,2,4-triazole analogues which are derived from corresponding carboxylic acid hydrazides. Some of the 1,2,4-triazoles have presented good inhibitory activity. For that reason, we believe that the 1,2,4-triazole scaffold could be a promising start for the further improvement in inhibitory activity of thymidine phosphorylase. To identify the binding affinities of synthesized 1,2,4-triazoles required for the potential thymidine phosphorylase inhibitory activity, docking study of compounds **3a–3l** and **4a–4g** to thymidine phosphorylase enzyme was performed with the Sybyl-X and PyMOL software.

2. Results and discussion

2.1. Chemistry

Carboxylic acid hydrazide **1** was prepared by treating corresponding carboxylic ester with hydrazine monohydrate in the presence of ethanol under reflux reaction conditions for five hours (Scheme 1). Carboxylic acid hydrazide **1** and benzoyl isothiocyanate in toluene were stirred at room temperature for about 2 h to give pure benzoyl thiosemicarbazide **2** in quantitative yield (Scheme 1). Benzoyl thiosemicarbazide **2** was refluxed with 4 N NaOH for about 4 h and followed by neutralization to afford a pure white solid 5-phenyl-3-mercapto-4*H*-1,2,4-triazole **3a** in 86% yield (Scheme 1). During the optimization of the reaction

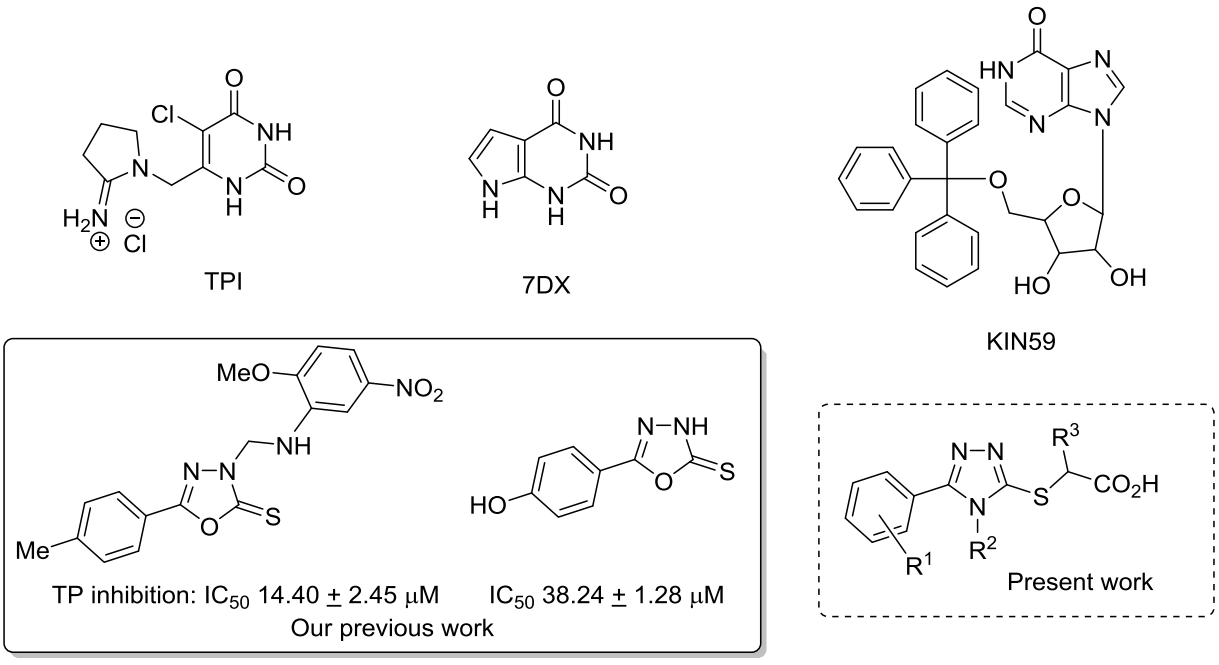

Fig. 1. Recently reported potent TP inhibitors and our ongoing work.

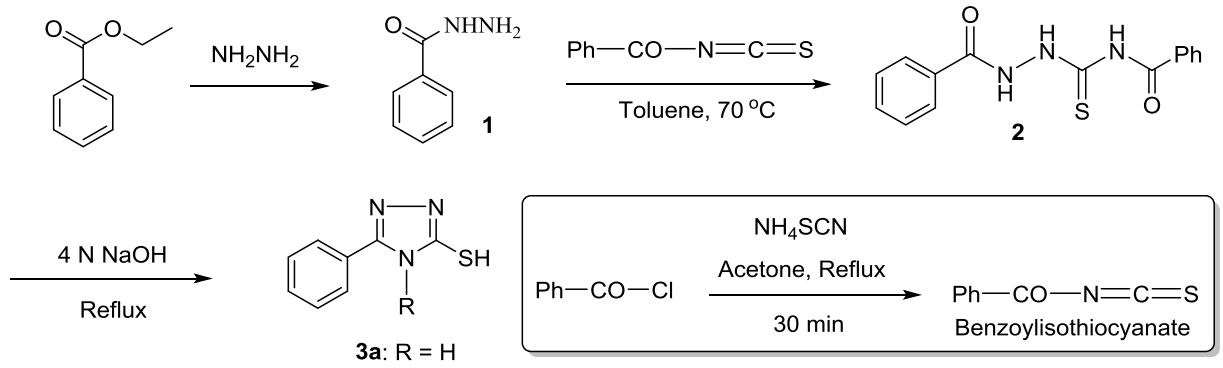

Scheme 1. Synthesis of benzoyl isothiocyanate and 3-mercapto-1,2,4-triazole **3a** from benzoylthiosemicarbzide **2**.

conditions, amount of NaOH, temperature and reaction time were surveyed for the optimum intramolecular cyclization of benzoyl thiosemicarbazide for the construction of 1,2,4-triazole. Under the optimized experimental reaction conditions, intramolecular cyclization of benzoyl thiosemicarbazide **2** in the presence of 4 N NaOH afforded mercapto-1,2,4-triazole **3a** in good yield (Scheme 1). The intramolecular cyclization of benzoyl thiosemicarbazide **2** typically requires harsher reaction conditions (4 N NaOH). In fact, base mediated intramolecular cyclization and hydrolysis of amide functionality *N*-benzoyl group at the 4-position of the 1,2,4-triazole could be accomplished in same step under prolonged reaction conditions (Scheme 1).

As expected, treatment of benzohydrazide **1** with ammonium thiocyanate in refluxing ethanol in the presence of HCl, gave 4*H*-5-mercapto-3-phenyl-1,2,4-triazole **3a–3e** as shown in Scheme 2. However, compound **3a** was also formed from base mediated-intramolecular cyclization of 1,4-dibenzoyl-thiosemicarbazide **2** under prolonged reaction conditions (Scheme 1).

By reacting mercapto-1,2,4-triazoles **3a–3e** with chloro or bromo substituted acetic acid at room temperature, title compound carboxylic acid substituted 3-mercapto-1,2,4-triazoles **4a–4g** were obtained as a white solid in 71–90% yields (Scheme 2). The procedure does not require any anhydrous solvent and inert atmosphere. No chromatographic purification was required, and all synthesized compounds were purified through simple recrystallization (Scheme 2).

In search to find more convenient route for the synthesis of 5-mercapto-1,2,4-triazole, benzoylation of thiosemicarbazide was also adopted. Simple benzoylation of thiosemicarbazide **6** with benzoyl chloride in the presence of pyridine, gave desired thiosemicarbazide **5** but in poor yield (Scheme 3). In order to identify improved procedure for benzoylation of benzohydrazide, simple benzohydrazide was selected to optimize the reaction conditions such as effects of various solvents ad reaction temperature but yield was not improved after several attempts due to formation of more than one product of benzoylation. Further intramolecular cyclization of thiosemicarbazide **5** in the presence of 4 N NaOH was refluxed for appropriate time followed by neutralization with 4 N HCl to afford a pure white solid 5-phenyl-3-mercapto-4*H*-1,2,4-triazole **3a** in 91% yield. However, this synthetic sequence for the construction of desired 3-mercapto-1,2,4-triazole was not efficient due to inadequate benzoylation of thiosemicarbazide **6** (Scheme 3).

When reaction of a variety of hydrazides **1f–1l** with phenyl isothiocyanate was carried out in the presence of toluene at 70 °C, different thiosemicarbazides **7f–7l** was formed in good yields. Upon refluxing of the obtained thiosemicarbazides **7f–7l** with aqueous sodium hydroxide, respective 1,2,4 – triazoles **3f–3l** were formed in 70–83% yields through intramolecular cyclization of corresponding thiosemicarbazides (Scheme 4).

All synthesized compounds were characterized using spectroscopic techniques such as ^{1}H NMR, ^{13}C NMR and IR spectroscopy. Chemical structures were further confirmed by mass spectrometry analysis.

2.2. Biological activity

The 1,2,4-triazole-3-thiol and its analogues can be considered as another class of inhibitors with encouraging inhibitory activities against angiogenic enzyme thymidine phosphorylase. To our knowledge, 1,2,4-triazole analogs are first time identified as inhibitors of thymidine phosphorylase. Moreover, these findings can be further explored and optimized in rational design of potent thymidine phosphorylase inhibitors. Thymidine phosphorylase inhibitory potential of synthesized compounds **3a–3l** and **4a–4g** were assessed using a literature procedure [41]. The inhibitory activity is presented in terms of IC_{50} values. The 7-Deazaxanthine (7DX) was used as a reference inhibitor with IC_{50} = 38.68 ± 4.42 µM.

Eleven out of nineteen 1,2,4-triazole analogs for instance **3b**, **3c**, **3f**, **3k**, **3l**, and **4b–4g** exhibited thymidine phosphorylase inhibitory activity. In the first series of 1,2,4-triazole analogs, compound **3b** and **3l** demonstrated good thymidine phosphorylase inhibitory activity (Table 1, entry 2 and 12). In the second series of 1,2,4-triazole analogs, compounds **4c**, **4d**, and **4g** displayed good inhibitory activity (Table 2,

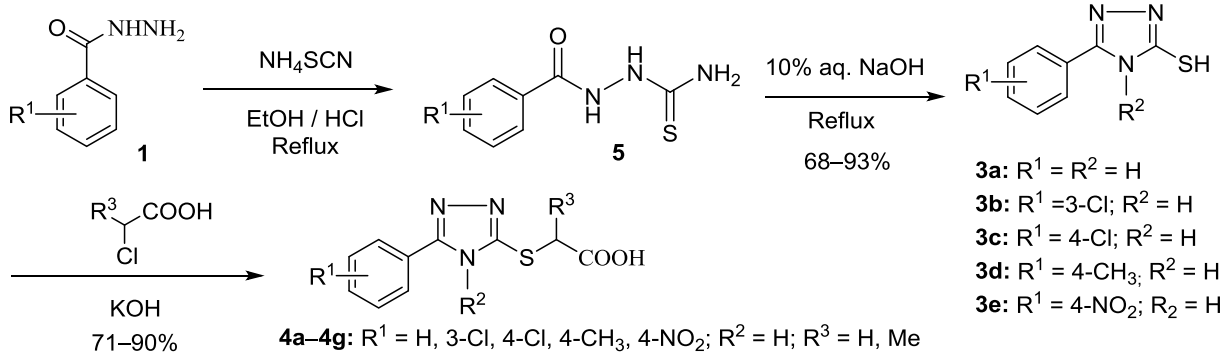

Scheme 2. Synthesis of 3-mercapto-1,2,4-triazole analogues (**3a–3e**) and 3-mercapto-1,2,4-triazole carboxylic acids (**4a–4g**).

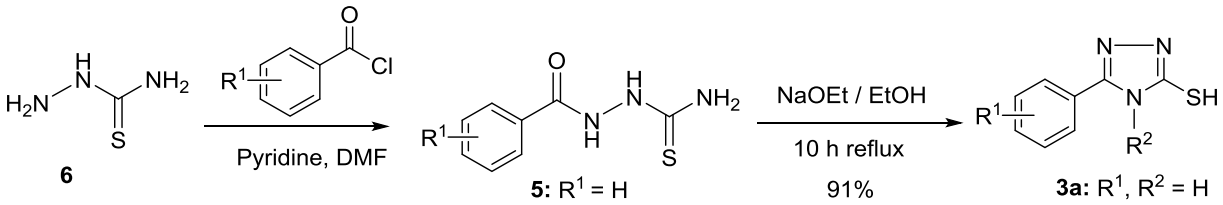

Scheme 3. Attempt towards convenient and efficient synthesis of 3-mercapto-1,2,4-triazole **3a**.

entry 3, 4 and 7). The structure activity relationship (SAR) for TP inhibitory potential is critically depends on substitution patterns on phenyl ring and triazole ring system. It was observed that all those analogs having either chloro substituted phenyl ring or nitrogen incorporated pyridyl group displayed thymidine phosphorylase inhibition (Table 1, entry 2, 3, 11 and 12). However, no inhibitory activity was observed in compounds **3a**, **3d**, **3e**, **3g–3j** and **4a**. The absence of inhibitory activity might be due to non-availability of chloro group on 5-substituted phenyl ring (Table 1, entry 1, 4 and 5). Among 1,2,4-triazoles **3a–3e** without phenyl group at the position **4** of 1,2,4-triazoles, only chloro substituted phenyl at the position 5 of 1,2,4-triazoles **3b** and **3c** exhibited good inhibitory activity with IC_{50} value 61.98 ± 0.43 and 187.60 ± 2.17 μM respectively. Compounds **3k** and **3l** having pyridyl functionality displayed modest inhibitory activity with IC_{50} value of 112.34 ± 0.76 and 82.32 ± 0.76 respectively.

Further increase in inhibitory activity was noticed in thiol functionalized analogs **4b–4g**. The better potential displayed by thiol functionalized analogs is owing to the presence of carboxylic acid. This polar functional group may meticulously interact with the target enzyme through hydrogen bonding. It was noticed that position of substituent on aromatic ring and exact nature of carboxylic acid greatly influenced the inhibitory potential of synthesized analogues. The greater inhibitory potential was revealed by compound **4d** than **4b**, **4c** and **4e** which are based on the position of chloro group on phenyl moiety. Moreover, dramatically increased inhibitory potential of compound **4d** with IC_{50} value 43.86 ± 1.11 μM was greatly influenced by steric bulk of R^3 around carboxylic acid moiety. The enormous activity difference among these analogs **4b–4e** displayed that position of chloro group on aromatic ring and presence of R^3 (either H or Me) greatly influences the inhibition which clearly demonstrates a significant role in this inhibition. Impact of other substituents such as methyl or nitro on phenyl moiety (analogs **4f** and **4g**) was also investigated. The nitrophenyl substituted triazole **4g** displayed potent inhibition with IC_{50} of 64.54 ± 5.62 μM. Finally, molecular docking analysis was performed to further investigate detailed triazole-enzyme binding interaction.

Table 1
Inhibition of thymidine phosphorylase by 1,2,4-triazole-3-thiols **3a–3l**.

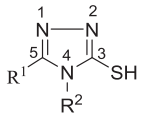

Entry	Compound	R^1	R^2	IC_{50} (μM)
1	**3a**	Phenyl	H	–
2	**3b**	3-Chlorophenyl	H	61.98 ± 0.43
3	**3c**	4-Chlorophenyl	H	187.60 ± 2.17
4	**3d**	4-Methylphenyl	H	–
5	**3e**	4-Nitrophenyl	H	–
6	**3f**	Phenyl	Phenyl	273.43 ± 0.96
7	**3g**	4-Methylphenyl	Phenyl	–
8	**3h**	3,4,5-Trimethoxyphenyl	Phenyl	–
9	**3i**	3-Chlorophenyl	Phenyl	–
10	**3j**	4-Chlorophenyl	Phenyl	–
11	**3k**	3-Pyridyl	Phenyl	112.34 ± 0.76
12	**3l**	4-Pyridyl	Phenyl	82.32 ± 0.76

Table 2
Inhibitory activity of 1,2,4-triazole-3-mercaptocarboxylic acids **4a–4g**.

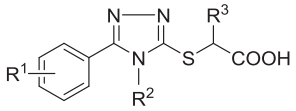

Entry	Compound	R^1	R^2	R^3	IC_{50} (μM)
1	**4a**	H	H	H	–
2	**4b**	3-Cl	H	H	163.43 ± 2.03
3	**4c**	3-Cl	H	CH_3	94.63 ± 4.28
4	**4d**	4-Cl	H	H	43.86 ± 1.11
5	**4e**	4-Cl	H	CH_3	220.55 ± 3.86
6	**4f**	4-CH_3	H	H	143.76 ± 1.12
7	**4g**	4-NO_2	H	H	64.54 ± 5.62

2.3. Docking studies

Structure of thymidine phosphorylase (TP) isolated from *Escherichia coli* (PDB code: 4EAD; resolution: 1.50 Å) in a complex with ONP (3′-azido-2′-fluoro-dideoxyuridine) has been used in order to analyze the binding mode of two novel series of 1,2,4-triazole derivatives. The protein complex used for studies was prepared, and docking was performed according to the previously described method [39]. Validation was carried out based on two reference compounds – TPI (5-chloro-6-[(2-iminopyrrolidin-1-yl)methyl]uracil) and ONP which were crystallized in complexes with TP. Obtained results of validation process (low RMSD values) have shown that docking parameters used for reproduction of original arrangement of the ligands were set correctly. Docking studies included also 7DX (7-deazaxanthine) – assay compound used in inhibition in vitro studies. After docking 7DX, its interactions within protein binding site were the same as previously [40]. Calculation of pKa values has shown that ligands from two 1,2,4-triazole series in physiological conditions are present in ionized form

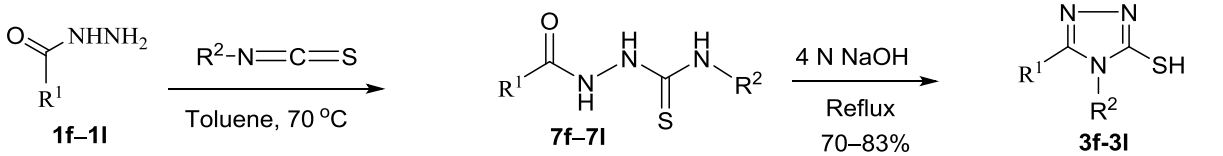

Scheme 4. Synthesis of 1,2,4-triazole-3-thiols (**3f–3l**) using phenyl isothiocyanate and corresponding hydrazides.

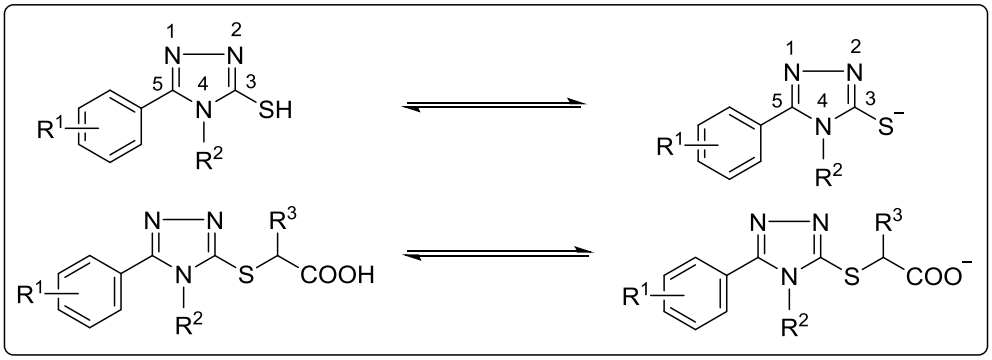

Fig. 2. Dissociation process for tested compounds **3a–3l** and **4a–4g**.

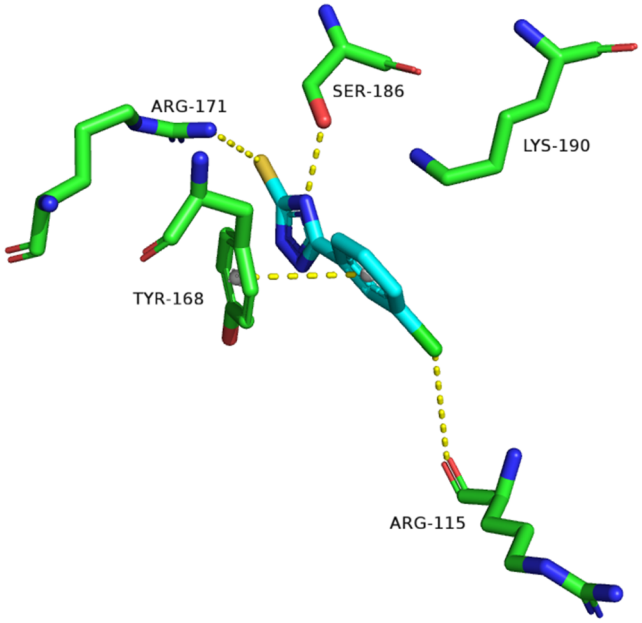

Fig. 3. Binding mode of compound **3b** within the active site of *E. coli* thymidine phosphorylase. The most important contacts between ligand and protein are shown as yellow dashes.

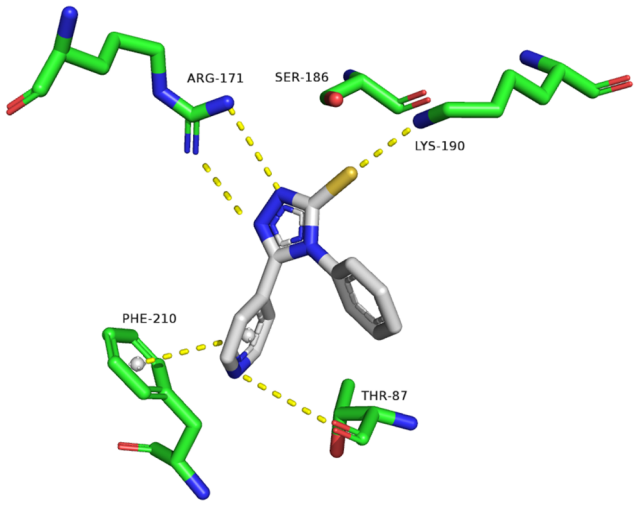

Fig. 4. Binding mode of compound **3l** within the active site of *E. coli* thymidine phosphorylase. The most important contacts between ligand and protein are shown as yellow dashes.

(Fig. 2). However, dissociation degree is higher for carboxylic acids (the second series).

All compounds of the first series were docked into the active site of enzyme, and thiolate group of almost all derivatives interacted with Arg171. One exception was compound **3l** with 4-pirydyl substituent. The most active compound from the first series of derivatives was **3b** (Fig. 3) which interacted with protein binding pocket as follows: thiolate group created ionic and hydrogen bonds with Arg171. Nitrogen atom in position 4 of triazole ring interacted by H-bond with Ser186. Chlorine atom in position 3 of phenyl ring interacted with Arg115 by halogen bond. Phenyl substituent created π-π interactions with Tyr168. Superposition of inactive compound **3a** and the most active **3b** showed similar arrangement in the active site of enzyme. It seems that halogen atom in aromatic substituent could trigger stronger interaction with the enzyme. The second most active compound from the first series was **3l** (Fig. 4) which has 4-pyridyl instead of substituted phenyl moiety. Binding mode of **3l** was different than other 1,2,4-triazole derivatives. Thiolate group interacted with Lys190. Nitrogen atoms in position 1 and 2 of triazole ring were engaged in hydrogen bonds with Arg171 guanidine group. Pyridine aromatic ring created weak π-π interactions with Phe210 while its nitrogen atom interacted with Thr87 by H-bond.

The compounds of the second series **4a–4g** revealed upon docking a characteristic binding mode where an ionized carboxyl group of all derivatives interacted with Arg171 through ionic bond. The phenyl group of the most active compound **4d** created weak π-π interactions (Fig. 5), while the chlorine atom in 4 position interacted with His119 through halogen bond. Comparing the most active compound **4d** and **4a** with no significant inhibitory activity it could be observed that both derivatives had similar binding mode. On the other hand, the presence of appropriate substituent (e.g. chlorine atom for compound **4d**) in aromatic ring, which created additional interactions with the amino acid residues of binding pocket, was essential and must be emphasized.

Summing up, the most important structural features, which provided significant increase in inhibitory activity of 1,2,4-triazole derivatives, were carboxyl group in the side chain due to creation of ionic bond and halogen atom or nitro group in phenyl substituent because of halogen or hydrogen bonds, respectively.

2.4. *In vivo* studies

To further verify the results of thymidine phosphorylase enzyme inhibition activity of triazole acid **4d**, *in vivo* studies were planned. For this, porous hydrogels of chitosan (CS) were prepared by freeze gelation and variable concentrations (1 mg, 3 mg and 6 mg) of **4d** were loaded on these hydrogels by physical adsorption technique. These hydrogels were given the codes CS-1, CS-3 and CS-6, depending upon the amount of **4d** loaded on each hydrogel. In present study, these three different concentrations of triazole acid **4d** were compared to examine its influence on the morphology, thermal stability, biodegradation, and biocompatibility of prepared hydrogels.

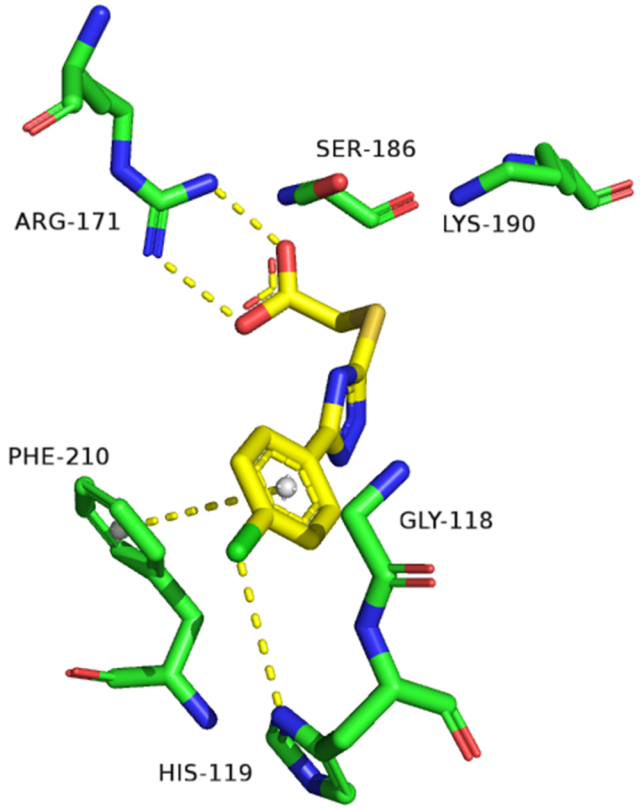

Fig. 5. Binding mode of compound **4d** within the active site of *E. coli* thymidine phosphorylase. The most important contacts between ligand and protein are shown as yellow dashes.

The hydrogels were carefully neutralized using NaOH solution. The porosity of the hydrogels was confirmed by taking SEM images of these scaffolds. The chemical nature of the loaded triazole scaffold was revealed by FTIR analysis. Typical photographs of the appearance of porous hydrogels loaded with triazole acid **4d** are displayed in Fig. 7. Further, these scaffolds were used to check their angiogenic behavior with reference to control which was devoid of any loaded drug, using *in vivo* chick chorioallantoic membrane (CAM) assay. This assay is used as a standard method to asses angiogenic behavior of a substance [41,42].

2.4.1. Structural analysis of hydrogels using Fourier-transform infrared (FTIR) spectroscopy

The IR spectrum of chitosan exhibited an intense characteristic absorption band at 3454 cm^{-1} owing to OH and N—H stretching vibrations (Fig. 6). Another distinctive peak at 2923 cm^{-1} showed presence of symmetric CH_2 stretching vibration of pyranose ring. The broad peak of C—O stretching vibration in chitosan was observed at 1021 and 1098 cm^{-1}. The appearance of characteristic absorption peaks at 1628 and 1540 cm^{-1} were attributed to corresponding C═O stretching of amide I and NH stretching of amide II, respectively. The characteristic anti-symmetric stretching absorption bands of C—O—C bridge was observed at 1151 cm^{-1}. The appearance of stretching absorption bands at 1098 and 1021 cm^{-1} were clearly attributed to the skeletal vibrations of C—O ether linkage (Fig. 6).

2.4.2. Assessment of morphology of hydrogels through scanning electron microscopy (SEM)

The surface morphology of freeze-gelated triazole acid **4d** loaded hydrogels was analyzed using scanning electron microscopy (SEM) that revealed highly porous nature of these hydrogels. It is well recognized that the microstructure of hydrogels affects cell behavior and aids in cell infiltration, adhesion, proliferation, when used in a biological system in tissue engineering. The microstructure of CS scaffolds with and without triazole loading are portrayed in Fig. 7. The hydrogels without triazole (CS) acid **4d** acted as control to observe any changes caused by triazole loading. It was observed that triazole loading did not disturb open-pore morphology of hydrogels and porous structure of the hydrogel scaffolds was retained. All hydrogels exhibited well-interconnected porous channels. Interestingly, all hydrogels (CS, CS-1, CS-3, CS-6) demonstrated pore size in range of 25–55 μm ± 10.87 μm.

The SEM analysis also reinforced the finding from CAM assay that difference in angiogenic activity was exclusively observed due to change in the concentration of triazole acid **4d**. Pore-size of hydrogels did not play role in finding anticancer potential using CAM assay as all the hydrogels bore same pore-sizes and morphologies.

2.4.3. Swelling capacity of hydrogels

The higher capacity of a hydrogel to absorb water is a highly desirable for skin tissue engineering. The swelling capacity was investigated by soaking freshly prepared hydrogels in phosphate buffer saline (PBS) solution for 1–24 h. The swelling ratios of the scaffolds are shown in Fig. 8. The lower swelling ability of the control (without triazole loaded) scaffold was observed. In contrast, higher swelling of the triazole loaded scaffolds CS-1, CS-3 and CS-6 was clearly observed. There was no significant difference in swelling between CS-1 and CS-3 scaffold. The water-binding ability of the chitosan/triazole acid loaded scaffold could be attributed to both their hydrophilicity and the maintenance of their three-dimensional structure. The swelling ability of the hydrogels CS-1 and CS-3 increases. The swelling ability is concentration dependent because it dramatically decreases with increased concentration of loaded triazole CS-6 with the passage of time. The swelling studies were supported by SEM results which displayed higher degree of cross-linking including slight decrease in average pore-size. Cross-linking is extremely important because it improves mechanical strength of hydrogels and helps to maintain their physical structure in media.

2.4.4. Assessment of angiogenic properties of hydrogels using CAM assay

Angiogenesis, a physiological process controlled by chemical signals in the body, is the formation of new blood vessels from pre-existing blood vessels. To ascertain the angiogenic response of the synthesized triazoles loaded hydrogels, chick chorionic allantoic membrane was executed on day 7 by creating a small window in the shell of chick embryos. One piece of triazoles loaded hydrogel of different concentration was entrenched in one egg (n¼10) and were hatched until day 14 of development. All the samples retrieved from the CAM assay after sacrificing the eggs were stabilized with paraformaldehyde and further dehydrated with ramp solution of ethanol (45–100%). On the basis of blood vessels, capability of triazoles loaded hydrogel were evaluated by taking the cross-section area of scaffolds and can also be assessed by CAM retrieved scaffold.

Cross section area of triazole acid **4d** loaded hydrogels with concentration of CS-1, CS-3 and CS-6 depicts greater antiangiogenic activity as depicted in Fig. 9. It was also confirmed by the CAM retrieved scaffold images that the surface of triazole acid loaded hydrogels showed greater inhibition in growth of blood vessels as compared to control which is deprived of triazole acid. This ultimately confirms the toxic behavior of triazole acid loaded biomaterials towards growing blood vessels.

3. Conclusion

In summary, various analogs of 1,2,4-triazole **3a–3l** and **4a–4g** were synthesized in good yields. All synthesized compounds were characterized using NMR spectroscopy and mass spectrometry. Inhibitory potential of synthesized compounds was evaluated against thymidine phosphorylase. Eleven compounds showed inhibitory activity against thymidine phosphorylase. Compound **4d** exhibited good inhibition

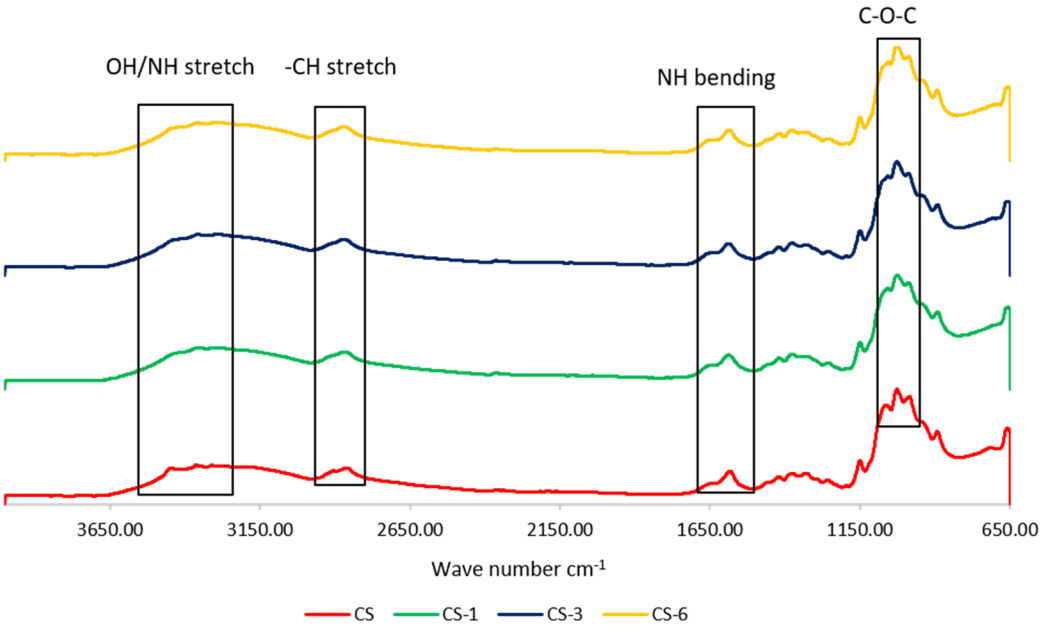

Fig. 6. FTIR spectra of CS, CS-1, CS-3 and CS-6.

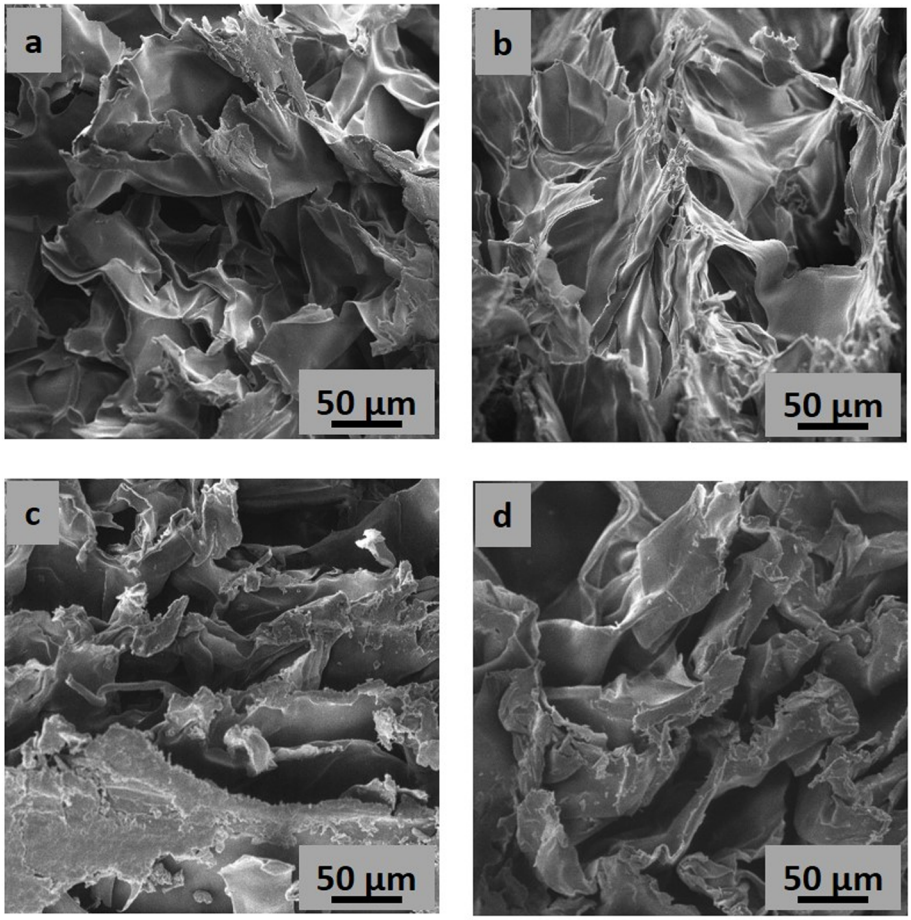

Fig. 7. SEM micrographs of (a) CS, (b) CS-1, (c) CS-3 and (d) CS-6 at a magnification of 500×.

against thymidine phosphorylase with IC_{50} = 43.86 ± 1.11 µM. Furthermore, angiogenic potential of compound **4d** was estimated using the chick chorionic allantoic membrane (CAM) assay. Molecular docking studies demonstrated characteristic binding interaction of the compounds to the enzyme. Current study may offer the suitable modification to design improved lead structure with increased inhibitory activity towards the enzyme.

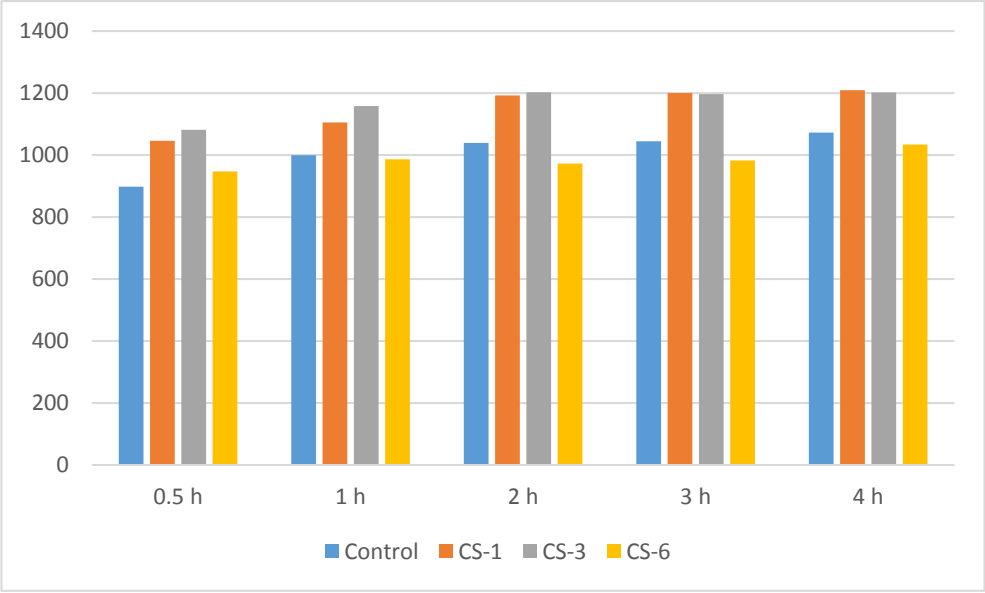

Fig. 8. Swelling properties of 1,2,4-triazole acid **4d**.

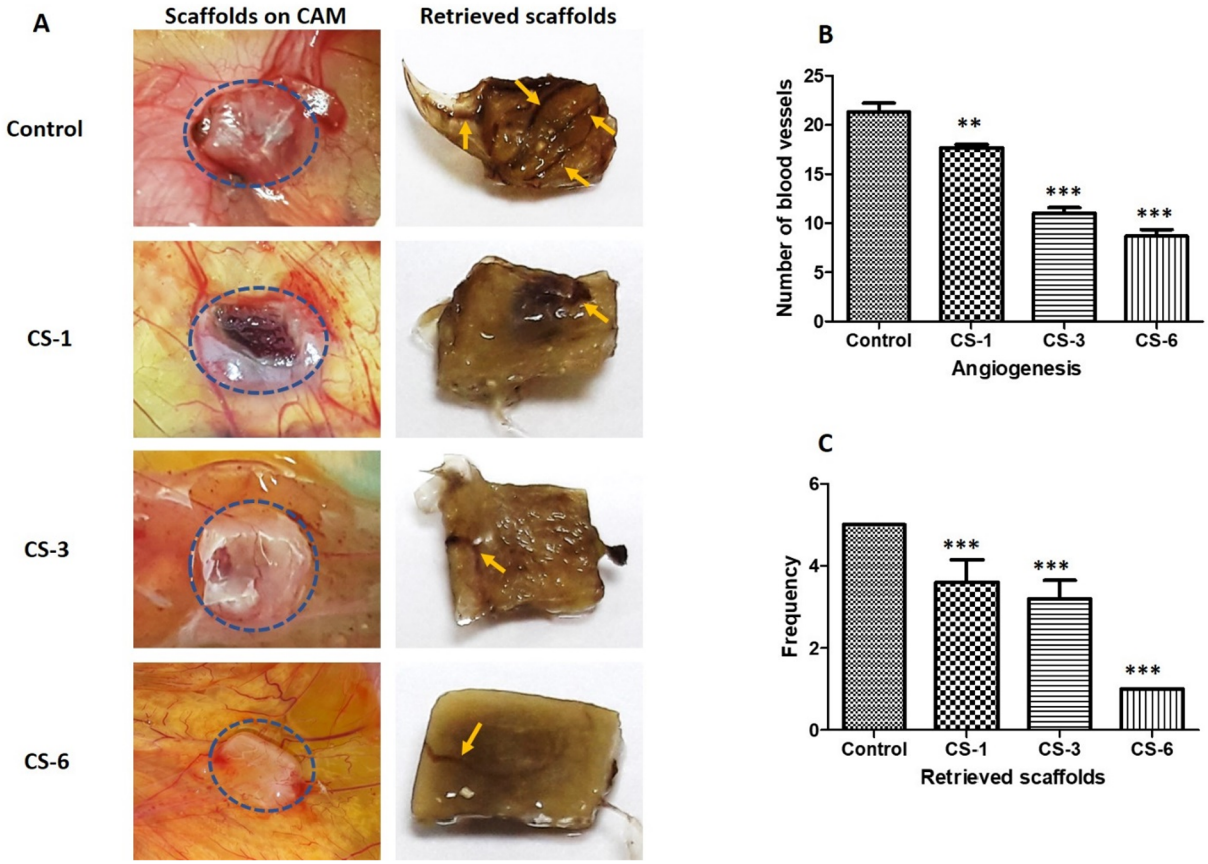

Fig. 9. [A] Evaluation of angiogenic potential of synthesized materials using CAM assay. The appearance of hydrogels on CAM (blue dotted circles showing position of hydrogels on the CAM) and retrieved hydrogels at day 14 is shown. Yellow arrows indicating the blood vessels inside the ex-planted scaffolds [B] Quantitative evaluation of angiogenic potential of synthesized materials using CAM assay. These hydrogels were placed on CAM for 7 days and the light microscope images were taken. The results are ± S.D of 4 viable chicks surviving from original group of 7 fertilized eggs per group. A circle (1 mm away from scaffold) was drawn around the hydrogel and blood vessels inside the circle were counted for quantification of angiogenesis. [C] Histogram of the blindly scored blood vessels in retrieved scaffolds. The comparison of control group with with all other groups (CS-1, CS-3 and CS-6) indicated significant difference between these two groups (*** $P < 0.05$).

4. Materials and methods

NMR spectra were attained at 400 MHz using BRUKER NMR spectrometer in $CDCl_3$ and DMSO-d_6. Chemical shifts were measured relative to TMS as an internal standard. Mass spectra were obtained on Bruker Mass spectrometer (Bruker Daltonic flex analysis). CHN Analysis was performed on a Carlo Erba Strumentazion-Mod-1106, Italy. Infrared (IR) spectra were recorded on JASCO IR-A-302 spectrometer as KBr (disc). Thin layer chromatography (TLC) was carried out on precoated silica gel aluminum plates (Kieselgel 60, F254, Merck, Germany). Chromatograms were seen under UV at 254 and 365 nm. Chitosan (CS) was received from Mian Scientific Company (Lahore, Pakistan) and processed for further purification at laboratory. Glacial acetic acid was obtained from Analar BDH Laboratory Supplies, UK. Sodium hydroxide was taken from Sigma Aldrich. All other chemicals were obtained from Oakwood Chemicals (USA) and Alfa Aesar (USA).

4.1. Docking studies

All input structures and docking runs were set according to the previously described method [39,40]. The spatial structures of ligands were prepared in Corina Online (Molecular Networks). Gasteiger-Marsili atomic partial charges were assigned in Sybyl-X software. Available in Protein Data Bank thymidine phosphorylase structure (code: 4EAD) was prepared in the following way: at the beginning sulfate ion in the active site was replaced by dihydrogen phosphate, and then using Hermes desktop software histidine residues were protonated at Nε, finally the binding site was defined as all amino acid residues that stayed in the range of 10 Å from reference ligand ONP. All water molecules within the distance of 5 Å from ONP has been taken into account during the ligand docking with attribute “toggle”. Docking process was performed by Gold 5.1 software and standard parameters of genetic algorithm were applied with population size 100 and operation number 100,000. Ten poses of each ligand were obtained and evaluated by GoldScore fitness function. Results were visualized using PyMOL software.

4.2. Thymidine phosphorylase assay

A commercially available E. coli TP (sigma T6632) was used because of less accessibility of human TP. Activity of recombinant E. coli TP was evaluated by recording the absorbance at 290 nm spectrophotometrically. The original assay described by Krenitsky and Bushby was modified [43]. In short, a volume of 200 µL of reaction mixture was taken to perform biological assay. An entire volume of reaction mixture contained 145 µL of potassium phosphate buffer (pH 7.4), 30 µL of enzyme (E. coli, sigma T6632) at concentration 0.05 and 0.002 U, respectively. The resulting reaction mixture was incubated with target compounds (5 µL) for 10 min at 25 °C in microplate reader. After incubation, pre read at 290 nm was used to infer the absorbance of substrates. The 1.5 mM concentration of substrate (20 µL) was dissolved in potassium phosphate buffer. The resulting solution was instantly placed to plate. The reading was continuously measured after 10, 20, and 30 min in micro-plate reader (SpectraMax Plus 384). The 96-wells plate was used, and value of blank well was deducted from experimental wells to eradicate the background absorbance. All assay experiments were carried out in triplicate.

4.3. Preparation of CS membrane

To investigate the proangiogenic response of the hydrogels loaded with drug, chick chorionic allantoic membrane-based assay is performed. To investigate the biological potential (proangiogenesis and antiangiogenesis activity) of synthesized small organic molecules which are described in Scheme 2. The following procedure was adopted.

Chitosan (2.5 g) was dissolved in acetic acid (0.5 M, 100 ml). The solution was stirred for few hours followed by the simultaneous addition of drug molecule. The resulting solution was poured into petri dishes, and freezed at −20 °C for 12 h. The frozen solution was immersed in 3.0 M alkaline solution of ethanol precooled at −20 °C for few hours. 3.0 M alkaline solution of ethanol precooled at −20 °C was added to the frozen solution collected from the petri dishes. The hydrogels formed was washed with ethanol (50%), followed by absolute ethanol and then distilled water three times. The resulting hydrogels were dried at room temperature. The morphology of the hydrogels was studied by Scanning Electron Microscopy (SEM). The Fourier Transform Infrared (FT-IR) spectroscopic analysis of the hydrogels was also carried out.

4.4. Swelling properties

The swelling behaviour of the triazoles loaded hydrogels were investigated by dipping them in phosphate buffered saline (PBS). The samples were divided into small pieces of approximately equal weight and then submerged in PBS solution at 37 °C for 3 h. The samples were withdrawn after the intervals of 30 min, 1, 2, and 3 h and blotted dry and weighed again. The percentage degree of swelling was measured by following formula:

$$\text{Degree of swelling}\,(\%) = [(M_s - M_i)/M_i] \times 100$$

where M_s is the mass of hydrogel after swelling and M_i is the initial mass of the sample taken.

4.5. General procedures

4.5.1. General procedure for the synthesis of 5-substituted-4H-1,2,4-triazole-3-thiol (3a–3e)

Respective substituted hydrazides (20.0 mmol) **3a–3e** were dissolved in absolute ethanol (50 ml). The resulting solution of hydrazides was refluxed with ammonium isothiocyanate (30.0 mmol) in the presence of concentrated hydrochloric acid (10.0 ml) and ethanol for 5–6 h. The appeared precipitates of thiosemicarbazides **5a–5e** were filtered, washed and recrystallized from aqueous ethanol. Respective substituted thiosemicarbazides (5.0 mmol) **5a–5e** were added to 10% sodium hydroxide solution (25 ml) and allowed to reflux for 4–5 h. After cooling, reaction mixture was poured into ice-cold water. Then pH (5.0–6.5) was adjusted with dilute HCl. The resulting precipitates of 1,2,4-triazole-3-thiols **3a–3e** were filtered, washed and re-recrystallized from ethanol-water (1:3).

4.5.2. General procedure for the synthesis of 5-substituted-4-phenyl-4H-1,2,4-triazole-3-thiol (3f–3l)

Various substituted carboxylic acid hydrazides (25.0 mmol) and phenyl isothiocyanate (25.0 mmol) were dissolved in toluene (30 ml). The reaction mixture was heated for 1–2 h. After completion of the reaction, toluene was evaporated using a rotary evaporator. The resulting precipitates were filtered, washed with water, and recrystallized from ethanol. Recrystallized thiosemicarbazides **7** was further refluxed with 4 N sodium hydroxide for 4–5 h. After completion of cyclization, reaction mixture was acidified with dilute hydrochloric acid (adjusted pH 5–6). The resulting precipitates of 1,2,4-triazole-3-thiols **3f–3l** were collected through filtration, washed with water and recrystallized from ethanol.

4.5.3. General procedure for the synthesis of 2-[(5-substituted-4H-1,2,4-triazol-3-yl)thio]carboxylic acids (4a–4g)

5-Substituted-4H-1,2,4-triazole-3-thiols (5.0 mmol) **3** was dissolved in ethanolic solution of potassium hydroxide (pH 7.5–8.5). Then, 2-chloro substituted carboxylic acid (6.0 mmol) was added into solution of potassium salt of 1,2,4-triazole **3**. The resulting reaction mixture was stirred for 3 h at room temperature. The progress of reaction was monitored by thin layer chromatography. After completion of reaction,

reaction mixture was acidified using dilute hydrochloric acid (adjusted pH 6). Resulting precipitates were filtered, washed with water and recrystallized from aqueous ethanol. The resulting substituted-1,2,4-triazole carboxylic acids **4a–4g** were collected and recrystallized from ethanol.

*4.5.3.1. 5-Phenyl-4H-1,2,4-triazole-3-thiol **(3a)***. Yield: 93%, white solid; m.p. 255–256 °C. IR (cm^{-1}, KBr): 1485, 1571, 1612, 2598, 3007, 3355; ^{1}H NMR (400 MHz, DMSO-d_6): δ 7.52–7.53 (m, 3H, Ar-H), 7.91–7.93 (m, 2H, Ar-H), 13.68 (1H, s, NH) and 13.86 ppm (1H, s, NH). ^{13}C NMR (100 MHz, DMSO-d_6): δ 126.1, 126.2, 129.5, 131.0 (aromatic carbons), 150.9 (C-5), 167.5 (C-3). HRESI-MS: *m/z* calcd for $C_8H_7N_3S$ (M + H^+): 178.0439; found: 178.0450.

*4.5.3.2. 5-(3-chlorophenyl)-4H-1,2,4-triazole-3-thiol **(3b)***. ^{1}H NMR (400 MHz, DMSO-d_6) δ: 7.50–7.57 (m, 2H, Ar-H), 7.83–7.87 (m, 1H, Ar-H); 7.93 (s, 1H, Ar-H); 13.77 (bs, 1H, NH) ppm (1H, s). ^{13}C NMR (400 MHz, DMSO-d_6) δ: 111.6, 117.9, 126.8, 130.4, 133.6, 146.7, 152.3. HRESI-MS: *m/z* calcd for $C_8H_6N_3SCl$ (M + H^+): 212.0091; found: 212.0128.

*4.5.3.3. 5-(4-Chlorophenyl)-4H-1,2,4-triazole-3-thiol **(3c)***. Yield: 88%, white solid; m.p. 284–287 °C, IR (cm^{-1}, KBr): 1510, 1565, 1610, 2581, 3061, 3431; ^{1}H NMR (400 MHz, DMSO): 7.55 (d, 2H, Ar-H), 7.90 (d, 2H, Ar-H), 13.71 (1H, s, NH), 13.89 (1H, s, NH). ^{13}C NMR (100 MHz, DMSO): δ 125.3, 127.8, 129.6, 135.5, 150.4 (C-5), 167.8 (C-3). HRESI-MS: *m/z* calcd for $C_8H_6N_3SCl$ (M + H^+): 212.0081; found: 212.0136.

*4.5.3.4. 5-(4-Methylphenyl)-4H-1,2,4-triazole-3-thiol **(3d)***. Yield: 86%, white solid; m.p. 263–265 °C, IR (cm^{-1}, KBr): 1485, 1525, 1566, 1616, 2593, 2915, 3019, 3345; ^{1}H NMR (400 MHz, DMSO-d_6): δ 2.39 (s, 3H, Ar-CH_3) 7.29 (d, 2H, J = 8.1 Hz, Ar-H), 7.80 (d, 2H, J = 8.1 Hz, Ar-H), 13.63(s, 1H, NH) and 13.77 (s, 1H, NH). ^{13}C NMR (100 MHz, DMSO-d_6): δ 21.4 (CH_3) 124.3, 126.0, 130.0, 140.4, 152.1 (C-5), 167.5 (C-3). HRESI-MS: *m/z* calcd for $C_9H_9N_3S$ (M + H^+): 192.0592; found: 192.0614.

*4.5.3.5. 5-(4-Nitrophenyl)- 4H-1,2,4-triazole-3-thiol **(3e)***. Yield: 68%, brown-yellow solid; m.p. > 319 °C (lit. [44] m.p. > 320 °C). IR (cm^{-1}, KBr): 1519, 1567, 1612, 2589, 3060, 3381; ^{1}H NMR (400 MHz, DMSO-d_6): 8.15 (d, 2H, J = 7.9 Hz, Ar-H), 8.30 (d, 2H, J = 7.9 Hz, Ar-H), 13.53 (s, 1H, NH); ^{13}C NMR (100 MHz, DMSO): δ 124.1, 126.2, 129.1, 136.2, 151.2 (C-5), 167.1 (C-3). HRESI-MS: *m/z* calcd for $C_8H_6N_4O_2S$ (M + H^+): 223.0292; found: 223.0314.

*4.5.3.6. 4,5-Diphenyl-2,4-dihydro-3H-1,2,4-triazole-3-thione **(3f)***. Yield: 83%. IR (cm^{-1}, KBr): 1555, 1618, 2575, 3071, 3368; ^{1}H NMR (400 MHz, DMSO-d_6): δ 7.27–7.31 (m, 3H, Ar-H), 7.33–7.35 (m, 3H, Ar-H), 7.38–7.42 (m, 1H, Ar-H), 7.47–7.50 (m, 3H, Ar-H), 14.09 (1H, s, NH) ppm. EI MS: *m/z* (rel abund. %): 253 (M^+, 52), 252 (39), 194 (9), 193 (3), 150 (11), 149 (16), 118 (22), 103 (44), 104 (14), 91 (35), 77 (1 0 0), 65 (18), 64 (17), 63 (17), 51 (70). HRESI-MS: *m/z* calcd for $C_{14}H_{11}N_3S$ (M + H^+): 254.0739; found: 254.0750.

*4.5.3.7. 5-(4-Methylphenyl)-4-phenyl-2,4-dihydro-3H-1,2,4-triazole-3-thione **(3g)***. Yield: 81%. IR (cm^{-1}, KBr): 1557, 1607, 2572, 3073, 3378; ^{1}H NMR (400 MHz, DMSO-d_6): δ 7.11–7.18 (m, 4H, Ar-H), 7.30–7.33 (m, 2H, Ar-H), 7.46–7.49 (m, 3H, Ar-H), 14.05 (s, 1H, NH) ppm. EIMS (*m/z*, rel. abund. %): 267 (M^+, 100), 266 (78), 208 (11), 194 (7), 150 (7), 149 (19), 132 (16), 131 (15), 118 (17), 117 (22), 109 (8), 91 (37), 77 (68), 65 (22), 51 (24). HRESI-MS: *m/z* calcd for $C_{15}H_{13}N_3S$ (M + H^+): 268.0845.1001; found: 268.0849.

*4.5.3.8. 5-(3,4,5-Trimethoxyphenyl)-4-phenyl-2,4-dihydro-3H-1,2,4-triazole-3-thione **(3h)***. Yield: 71%. IR (cm^{-1}, KBr): 1560, 1613, 2582, 3064, 3372; ^{1}H NMR (400 MHz, DMSO-d_6): δ 3.52 (s, 6H, 3,5-$(OCH_3)_2$), 3.62 (s, 3H, OCH_3), 6.57 (s, 2H, Ar-H), 7.36–7.38 (m, 2H, Ar-H), 7.51–7.55 (m, 3H, Ar-H), 14.09 (s, 1H, NH) ppm. EI MS: *m/z* (rel abund. %): 343 (M^+, 54), 342 (16), 329 (4), 328 (10), 193 (15), 285 (2), 150 (32), 149 (13), 135 (22), 120 (21), 118 (14), 104 (7), 91 (18), 77 (1 0 0), 65 (21), 51 (37). HRESI-MS: *m/z* calcd for $C_{17}H_{17}N_3O_3S$ (M + H^+): 344.1001; found: 344.1011.

*4.5.3.9. 5-(3-Chlorophenyl)-4-phenyl-2,4-dihydro-3H-1,2,4-triazole-3-thione **(3i)***. Yield: 76%. IR (cm^{-1}, KBr): 1551, 1607, 2558, 3051, 3365; ^{1}H NMR (400 MHz, DMSO-d_6): δ 7.22–7.25 (m, 1H, Ar-H), 7.30–7.32 (m, 2H, Ar-H), 7.35–7.38 (m, 2H, Ar-H), 7.45–7.51 (m, 4H, Ar-H), 14.24 (s, 1H, NH) ppm. EIMS (*m/z*, rel. abund.%): 287 (M^+, 100), 289 (M^+ + 2, 37), 288 (50), 286 (92), 256 (2), 254 (3), 228 (7), 137 (5), 135 (7), 91 (6), 77 (18), 65 (3), 51 (8). HRESI-MS: *m/z* calcd for $C_{14}H_{10}ClN_3S$ (M + H^+): 288.0333; found: 288.0340.

*4.5.3.10. 5-(4-Chlorophenyl)-4-phenyl-2,4-dihydro-3H-1,2,4-triazole-3-thione **(3j)***. Yield: 79%. IR (cm^{-1}, KBr): 1553, 1608, 2557, 3054, 3366; ^{1}H NMR (400 MHz, DMSO-d_6): δ 7.29 (d, 2H, J = 6.8 Hz, Ar-H), 7.34–7.36 (m, 2H, Ar-H), 7.41 (d, 2H, J = 6.8 Hz, Ar-H), 7.48–7.50 (m, 3H, Ar-H), 14.17 (s, 1H, NH) ppm. EIMS (*m/z*, rel. abund.%): 287 (M^+, 100), 289 (M^+ + 2, 35), 288 (49), 286 (93), 256 (4), 254 (6), 228 (9), 137 (7), 135 (11), 91 (8), 77 (17), 65 (5), 51 (13). HRESI-MS: *m/z* calcd for $C_{14}H_{10}ClN_3S$ (M + H^+): 288.0333; found: 288.0339.

*4.5.3.11. 5-(3-Pyridyl)-4-phenyl-2,4-dihydro-3H-1,2,4-triazole-3-thione **(3k)***. Yield: 70%. IR (cm^{-1}, KBr): 1548, 1615, 2533, 3044, 3321; ^{1}H NMR (400 MHz, DMSO-d_6): δ 7.36–7.40 (m, 3H, Ar-H), 7.48–7.51 (m, 3H, Ar-H), 7.64–7.67 (m, 1H, Ar-H), 8.48–8.58 (m, 2H, Ar-H), 14.22 (s, 1H, NH) ppm. EIMS (*m/z*, rel. abund.%): 254 (M^+, 100), 253 (68), 221 (3), 195 (9), 194 (6), 150 (4), 149 (13), 119 (17), 118 (4), 104 (13), 92 (11), 91 (11), 78 (20), 77 (54), 65 (13), 52 (5), 51 (36). HRESI-MS: *m/z* calcd for $C_{13}H_{10}N_4S$ (M + H^+): 255.0613; found: 255.0618.

*4.5.3.12. 5-(4-Pyridyl)-4-phenyl-2,4-dihydro-3H-1,2,4-triazole-3-thione **(3l)***. Yield: 73%. IR (cm^{-1}, KBr): 1550, 1618, 2537, 3049, 3331; ^{1}H NMR (400 MHz, DMSO-d_6): δ 7.44 (m, 4H, Ar-H), 7.53–7.55 (m, 4H, Ar-H), 8.70 (m, 1H, Ar-H), 14.50 (s, 1H, NH) ppm. EIMS (*m/z*, rel. abund. %): 254 (M^+, 100), 253 (81), 221 (2), 195 (10), 194 (5), 150 (5), 149 (15), 119 (11), 118 (6), 104 (9), 92 (6), 91 (12), 78 (18), 77 (51), 65 (12), 52 (6), 51 (51). HRESI-MS: *m/z* calcd for $C_{13}H_{10}N_4S$ (M + H^+): 255.0613; found: 255.0619.

*4.5.3.13. 2-[(5-phenyl-4H-1,2,4-triazol-3-yl)thio]acetic acid **(4a)***. Yield: 90%. IR (cm^{-1}, KBr): 3300–2325 (COOH), 1704 (C═O); ^{1}H NMR (400 MHz, DMSO-d_6): δ 4.01 (s, 2H, CH_2), 7.51–7.54 (m, 3H, Ar-H), 7.97–7.99 (m, 2H, Ar-H), 13.91 (s, 1H, NH), 15.88 (s, 1H, COOH) ppm. HRESI-MS: *m/z* calcd for $C_{10}H_9N_3O_2S$ $[M-H]^-$ 234.0468; Found 234.0471.

*4.5.3.14. 2-[(5-(3-chlorophenyl)-4H-1,2,4-triazol-3-yl)thio]acetic acid **(4b)***. Yield: 87%. IR (cm^{-1}, KBr): 3300–2310 (COOH), 1743 (C═O); ^{1}H NMR (400 MHz, DMSO-d_6): δ 4.11 (s, 2H, CH_2), 7.55–7.68 (m, 2H, Ar-H), 7.98–8.02 (m, 1H, Ar-H); 8.06 (s, 1H, Ar-H) 13.91 (s, 1H, NH), 15.88 (s, 1H, COOH) ppm. HRESI-MS: *m/z* calcd for $C_{10}H_8N_3O_2S$ $[M-H]^-$ 268.0068; Found 268.0272.

*4.5.3.15. 2-[(5-(3-chlorophenyl)-4H-1,2,4-triazol-3-yl)thio]propanoic acid **(4c)***. Yield: 78%. IR (cm^{-1}, KBr): 3300–2340 (COOH), 1742 (C═O); ^{1}H NMR (400 MHz, DMSO-d_6): δ 1.55 (d, 3H, CH_3), 4.19 (q, 1H,

CH), 7.56–7.68 (m, 2H, Ar-H), 7.97–8.01 (m, 1H, Ar-H); 8.05 (s, 1H, Ar-H) 13.86 (s, 1H, NH), 15.81 (s, 1H, COOH) ppm. HRESI-MS: *m/z* calcd for $C_{11}H_{10}ClN_3O_2S$ $[M-H]^-$ 282.0267; Found 282.0262.

4.5.3.16. 2-[(5-(4-chlorophenyl)-4H-1,2,4-triazol-3-yl)thio]acetic acid ***(4d)***. Yield: 88%. IR (cm^{-1}, KBr): 3300–2328 (COOH), 1745 (C=O); ^1H NMR (400 MHz, DMSO-d_6): δ 4.09 (s, 2H, CH_2), 7.55–7.63 (m, 2H, Ar-H), 8.02–8.06 (m, 2H, Ar-H), 14.32 (s, 1H, NH), 15.97 (s, 1H, COOH) ppm. HRESI-MS: *m/z* calcd for $C_{10}H_8ClN_3O_2S$ $[M-H]^-$ 268.0068; Found 268.0074.

4.5.3.17. 2-[(5-(4-chlorophenyl)-4H-1,2,4-triazol-3-yl)thio]propanoic acid ***(4e)***. Yield: 79%. IR (cm^{-1}, KBr): 3300–2305 (COOH), 1745 (C=O); ^1H NMR (400 MHz, DMSO-d_6): δ 1.54 (d, 3H, CH_3), 4.21 (q, 1H, CH), 7.58–7.68 (m, 2H, Ar-H), 8.03–8.07 (m, 2H, Ar-H), 14.02 (s, 1H, NH), 15.95 (s, 1H, COOH) ppm. HRESI-MS: *m/z* calcd for $C_{11}H_{10}ClN_3O_2S$ $[M-H]^-$ 282.0268; Found 282.0073.

4.5.3.18. 2-[(5-(4-methylphenyl)-4H-1,2,4-triazol-3-yl)thio]acetic acid ***(4f)***. Yield: 91%. IR (cm^{-1}, KBr): 3300–2301 (COOH), 1739 (C=O); ^1H NMR (400 MHz, DMSO-d_6): δ 3.93 (s, 2H, CH_2), 7.81 (d, 2H, J = 8.1 Hz, Ar-H), 7.98 (m, 2H, J = 8.1 Hz, Ar-H), 11.03 (s, 1H, NH), 15.84 (s, 1H, COOH) ppm. HRESI-MS: *m/z* calcd for $C_{11}H_{11}N_3O_2S$ $[M-H]^-$ 248.0631; Found 248.0638.

4.5.3.19. 2-[(5-(4-nitrophenyl)-4H-1,2,4-triazol-3-yl)thio]acetic acid ***(4g)***. Yield: 71%. IR (cm^{-1}, KBr): 3300–2309 (COOH), 1731 (C=O); ^1H NMR (400 MHz, DMSO-d_6): δ 4.31 (s, 2H, CH_2), 8.16 (d, 2H, J = 7.9 Hz, Ar-H), 8.31 (d, 2H, J = 7.9 Hz, Ar-H), 13.91 (s, 1H, NH), 15.88 (s, 1H, COOH) ppm. HRESI-MS: *m/z* calcd for $C_{10}H_8N_4O_4S$ $[M-H]^-$ 279.0341; Found 279.0347.

4.6. In vivo studies

4.6.1. Assessment of morphology of hydrogels through scanning electron microscopy (SEM)

The surface morphology of hydrogels without any triazole and with triazole 4d loading was investigated using SEM. The samples of different concentration of triazole acid 4d were loaded on a stub with conducting copper tape with a Nova NanoSEM-450. The SEM was carried out at 10 kV under low vacuum mode at 50 Pa. The pore size was measured using image processing software. The diameter of the pores was measured from an average of 30 arbitrarily chosen pores.

4.6.2. Structural analysis of hydrogels using Fourier-transform infrared (FTIR) spectroscopy

The functional groups and detailed structural analysis of the hydrogels was investigated by FTIR spectroscopy using Thermo Nicolet 6700P, USA. All spectra were measured in the range of 400–4000 cm^{-1} at 8 cm^{-1} spectral resolution and each spectrum is the average of 256 scans as depicted in Fig. 6.

4.6.3. Estimation of angiogenic potential of hydrogels using the chick chorionic allantoic membrane (CAM) assay

Freshly fertilized chicken eggs were acquired from Big bird Lahore (Pakistan). These fertilized eggs were incubated for 14 days at 37 °C in an egg incubator (RCOM Suro20) under humid environment. Digital pictures for evaluation of angiogenic potential using CAM assay is revealed in Fig. 9.

A miniature window (1 × 1 cm^2) was created in the shell at day 8. A small piece of hydrogel about 1 cm^2 was laid onto the chorionic allantoic membrane. The implanted small pieces of hydrogel were of about 1 × 1 cm^2. Each egg was implanted with one piece of hydrogel only. The shell window was exchanged with parafilm (Bemis Flexible Packaging, USA) and further sealed with adhesive tape. After implantation, eggs were placed again for 14 days in a 45% humidified incubator at 37 °C. At last, the eggs were sacrificed at day 14.

Angiogenesis was carefully evaluated and further quantified by taking light microscope pictures of the material on the CAM. In the end, hydrogels were detached for detailed analysis. Material of each group was added into 10 fertilized eggs. Typically, results obtained from surviving developing chicks were used. On average chick survival was found to be 80%.

Acknowledgement

The author (Dr. S. A. Shahzad) is very grateful to the Higher Education Commission (HEC) of Pakistan for providing financial support vide No. 5290/Federal/NRPU/R&D/HEC/2016.

Appendix A. Supplementary material

Supplementary data to this article can be found online at https://doi.org/10.1016/j.bioorg.2019.01.005.

References

[1] A. Esteban-Gamboa, J. Balzarini, R. Esnouf, E. De Clercq, M.-J. Camarasa, M.-J. Pérez-Pérez, J. Med. Chem. 43 (2000) 971–983.
[2] S. Tabata, M. Yamamoto, H. Goto, A. Hirayama, M. Ohishi, T. Kuramoto, A. Mitsuhashi, R. Ikeda, M. Haraguchi, K. Kawahara, Y. Shinsato, K. Minami, A. Saijo, M. Hanibuchi, Y. Nishioka, S. Sone, H. Esumi, M. Tomita, T. Soga, T. Furukawa, S.-I. Akiyama, Cell Rep. 19 (2017) 1313–1321.
[3] S.B. Fox, A. Moghaddam, M. Westwood, H. Turley, R. Bicknell, K.C. Gatter, A.L. Harris, J. Pathol. 176 (1995) 183–190.
[4] A. Bronckaers, F. Gago, J. Balzarini, S. Liekens, Med. Res. Rev. 29 (2009) 903–953.
[5] T. Furukawa, A. Yoshimura, T. Sumizawa, M. Haraguchi, S.-I. Akiyama, K. Fukui, M. Ishizawa, Y. Yamada, Nature 356 (1992) 668 668.
[6] A. Moghaddam, R. Bicknell, Biochemistry 31 (1992) 12141–12146.
[7] G. Barton, C. Ponting, G. Spraggon, C. Finnis, D. Sleep, Protein Sci. 1 (1992) 688–690.
[8] (a) I.V. Bijnsdorp, F. Capriotti, F.A.E. Kruyt, N. Losekoot, M. Fukushima, A.W. Griffioen, V.L. Thijssen, G.J. Peters, Br. J. Cancer 104 (2011) 1185–1192; (b) E.J. Yu, Y. Lee, S.Y. Rha, T.S. Kim, H.C. Chung, B.K. Oh, W.I. Yang, S.H. Noh, H.-C. Jeung, Mol. Cancer Res. 6 (2008) 1554–1566.
[9] A. Moghaddam, H.-T. Zhang, T. Fan, D.-E. Hu, V.C. Lees, H. Turley, S.B. Fox, K.C. Gatter, A.L. Harris, R. Bicknell, Proc. Natl. Acad. Sci. U.S.A. 92 (1995) 998–1002.
[10] K. Miyadera, T. Sumizawa, M. Haraguchi, H. Yoshida, W. Konstanty, Y. Yamada, S.-I. Akiyama, Cancer Res. 55 (1995) 1687–1690.
[11] S.-I. Akiyama, T. Furukawa, T. Sumizawa, Y. Takebayashi, Y. Nakajima, S. Shimaoka, M. Haraguchi, Cancer Sci. 95 (2004) 851–857.
[12] M.H. Iltzsch, M.H. El Kouni, S. Cha, Biochemistry 24 (1985) 6799–6807.
[13] I.V. Bijnsdorp, K. Azijli, E.E. Jansen, M.M. Wamelink, C. Jakobs, E.A. Struys, M. Fukushima, F.A. Kruyt, G.J. Peters, Biochem. Pharmacol. 80 (2010) 786–792.
[14] K.A. Hotchkiss, A.W. Ashton, E.L. Schwartz, J. Biol. Chem. 278 (2003) 19272–19279.
[15] N. Brown, R. Bicknell, Biochem. J. 334 (1998) 1–8.
[16] M. Haraguchi, K. Miyadera, K. Uemura, T. Sumizawa, T. Furukawa, K. Yamada, S. Akiyama, Y. Yamada, Angiogenic activity of enzymes, Nature 368 (1994) 198.
[17] M. Overman, G. Varadhachary, S. Kopetz, M. Thomas, M. Fukushima, K. Kuwata, A. Mita, R. Wolff, P. Hoff, H. Xiong, J. Abbruzzese, Invest. New Drugs 26 (2008) 445–454.
[18] M.A. Sajid, Z.A. Khan, S.A. Shahzad, S.A.R. Naqvi, M. Usman, A. Iqbal, Turk. J. Chem. 41 (2017) 1–28.
[19] (a) M.T. Javid, F. Rahim, M. Taha, M. Nawaz, A. Wadood, M. Ali, A. Mosaddik, S.A.A. Shah, R.K. Farooq, Bioorg. Chem. 79 (2018) 323–333; (b) I. Uddin, M. Taha, F. Rahim, A. Wadood, Bioorg. Chem. 78 (2018) 324–331; (c) H. Ullah, F. Rahim, M. Taha, I. Uddin, A. Wadood, S.A.A. Shah, R.K. Farooq, M. Nawaz, Z. Wahab, K.M. Khan, Bioorg. Chem. 78 (2018) 58–67; (d) M. Taha, S.A.A. Shah, M. Afifi, S. Imran, S. Sultan, F. Rahim, N.H. Ismail, K.M. Khan, Bioorg. Chem. 78 (2018) 17–23; (e) M. Taha, U. Rashid, S. Imran, M. Ali, Bioorg. Med. Chem. 26 (2018) 3654–3663.
[20] R.J. Mayer, E. Van Cutsem, A. Falcone, T. Yoshino, R. Garcia-Carbonero, N. Mizununa, K. Yamazaki, Y. Shimada, J. Tabernero, Y. Komatsu, New Engl. J. Med. 372 (2015) 1909–1919.
[21] P. Langen, G. Etzold, D. Bärwolff, B. Preussel, Biochem. Pharmacol. 16 (1967) 1833–1837.
[22] J. Balzarini, A.E. Gamboa, R. Esnouf, S. Liekens, J. Neyts, E. De Clercq, M.-J. Camarasa, M.-J. Pérez-Pérez, FEBS Lett. 438 (1998) 91–95.
[23] (a) E. Casanova, A.-I. Hernández, E.-M. Priego, S. Liekens, M.-J. Camarasa, J. Balzarini, M.-J. Pérez-Pérez, J. Med. Chem. 49 (2006) 5562–5570; (b) S. Liekens, A. Bronckaers, A.-I. Hernández, E.-M. Priego, E. Casanova, M.-J. Camarasa, M.-J. Pérez-Pérez, J. Balzarini, Mol. Pharmacol. 70 (2006) 501–509.

[24] D. Dheer, V. Singh, R. Shankar, Bioorg. Chem. 71 (2017) 30–54.
[25] (a) F.D.C. Da Silva, M.C.B.V. De Souza, I.I.P. Frugulhetti, H.C. Castro, S.L.D.O. Souza, T.M.L. De Souza, D.Q. Rodrigues, A.M.T. Souza, P.A. Abreu, F. Passamani, C.R. Rodrigues, V.F. Ferreira, Eur. J. Med. Chem. 44 (2009) 373–383; (b) M.J. Giffin, H. Heaslet, A. Brik, Y.C. Lin, G. Cauvi, C.-H. Wong, D.E. McRee, J.H. Elder, C.D. Stout, B.E. Torbett, J. Med. Chem. 51 (2008) 6263–6270.
[26] (a) S. Cocklin, H. Gopi, B. Querido, M. Nimmagadda, S. Kuriakose, C. Cicala, S. Ajith, S. Baxter, J. Arthos, J. Martin-Garcia, I.M. Chaiken, J. Virol. 81 (2007) 3645–3648; (b) A. Brik, J. Alexandratos, Y.C. Lin, J.H. Elder, A.J. Olson, A. Wlodawer, D.S. Goodsell, C.-H. Wong, ChemBioChem 6 (2005) 1167–1169.
[27] (a) W.J. Yu, Q. Rao, M. Wang, Z. Tian, D. Lin, X.R. Liu, J.X. Wang, Leukemia Res. 30 (2006) 575–582; (b) L.B. Peterson, Blagg S.J. Brian, Bioorg. Med. Chem. Lett. 20 (2010) 3957–3960.
[28] (a) M. Nahrwold, T. Bogner, S. Eissler, S. Verma, N. Sewald, Org. Lett. 12 (2010) 1064–1067; (b) J. Doiron, A.H. Soultan, R. Richard, M.M. Toure, N. Picot, R. Richard, M. Cuperlovic-Culf, G.A. Robichaud, M. Touaibia, Eur. J. Med. Chem. 46 (2011) 4010–4024.
[29] I. Fichtali, M. Chraibi, F.E. Aroussi, A. Ben-Tama, E.M.E. Hadrami, K.F. Benbrahim, S.E. Stiriba, Der. Pharma. Chem. 8 (2016) 236–242.
[30] B.F. Abdel-Wahab, H.A. Mohamed, G.E.A. Awad, Eur. Chem. Bull. 4 (2015) 106–109.
[31] Y.I. El-Gazzar, H.H. Georgey, S.M. El-Messery, H.A. Ewida, G.S. Hassan, M.M. Raafat, M.A. Ewida, H.I. El-Subbagh, Bioorg. Chem. 72 (2017) 282–292.
[32] M. Saeedi, M. Safavi, E. Karimpour-Razkenari, M. Mahdavi, N. Edraki, F.H. Moghadam, M. Khanavi, T. Akbarzadeh, Bioorg. Chem. 70 (2017) 86–93.
[33] B.D. Patel, S.V. Bhadada, M.D. Ghate, Bioorg. Chem. 72 (2017) 345–358.
[34] I. Khan, M.A. Tantray, H. Hamid, M.S. Alam, A. Kalam, F. Hussain, A. Dhulap, Bioorg. Chem. 68 (2016) 41–55.
[35] R.M. Shaker, Arkivoc ix (2006) 59–112.
[36] Yann Le Duc, Erol Licsandru, Daniela Vullo, Mihail Barboiu, Claudiu T. Supuran, Bioorg. Med. Chem. 25 (2017) 1681–1686.
[37] Sampark S. Thakkar, Parth Thakor, Hiren Doshi, Arabinda Ray, Bioorg. Med. Chem. 25 (2017) 4064–4075.
[38] D. Sarigol, A. Uzgoren-Baran, B.C. Tel, E.I. Somuncuoglu, I. Kazkayasi, K. Ozadali-Sari, O. Unsal-Tan, G. Okay, M. Ertan, B. Tozkoparan, Bioorg. Med. Chem. 23 (2015) 2518–2528.
[39] S.A. Shahzad, M. Yar, M. Bajda, B. Jadoon, Z.A. Khan, S.A.R. Naqvi, A.J. Shaikh, K. Hayat, A. Mahmmod, N. Mahmood, S. Filipek, Bioorg. Med. Chem. 22 (2014) 1008–1015.
[40] S.A. Shahzad, M. Yar, M. Bajda, L. Shahzadi, Z.A. Khan, S.A.R. Naqvi, S. Mutahir, N. Mahmood, K.M. Khan, Bioorg. Chem. 60 (2015) 37–41.
[41] L. Shahzadi, A.A. Chaudhry, A.R. Aleem, M.H. Malik, K. Ijaz, H. Akhtar, F. Alvi, A.F. Khan, I. Ur Rehman, M. Yar, Int. J. Biol. Macromol. 120 (2018) 721–728.
[42] J. Dewangan, S. Kaushik, S.K. Rath, A.K. Balapure, Life Sci. 193 (2018) 9–19.
[43] T.A. Krenitsky, S.R.M. Bushby, U.S. Patent, 4, 178, 212, 1–8, 1979.
[44] J. Wang, S. Haoxin, S. Haijian, Synth. Commun. 31 (2001) 2841–2848.